Earthquake Engineering, Tenth World Conference © 1992 Balkema, Rotterdam. ISBN 90 5410 060 5

Study on forward prediction model of earthquake ground motion for seismic design of structural systems

M. Kawano
Kyoto University, Japan

H. Dohi
Nippon Telegraph and Telephone Corporation, Tokyo, Japan

Y. Osada
Japan Airlines, Tokyo, Japan

T. Kobori
Kajima Corporation, Tokyo, Japan

ABSTRACT: This paper presents the theoretical model for forward prediction of ground motion on the basis of wave propagation in the two layered half space and source function which is expressed by the dynamic behavior of mass-spring system on the rough surface. To investigate the conditions as to refinement in wave propagation, site effect and source model, the verification of this simple theoretical model is developed through comparison with Miyagi-Oki earthquake data of June 12, 1976, which seems nearly close to a blind prediction test.

1 INTRODUCTION

The prediction of strong ground motion is very important for the establishment of the reasonable estimation of damage potential as well as the development of seismic design of structural systems. The several methods have been presented to simulate ground motion, in which the variety techniques are used in the backward process of idetifying the characteristics of the actual earthquake data. For forward prediction of ground motion, it is a great problem how to suppose the simplest possible representation of the ground motion model which can give adequate information for seismic design(Iwan, 1988), and how to select the key parameters which describe the essential correspondence between the characteristics of the ground motion model and the ones of actual earthquakes. From the above view point, in this paper, the theoretical ground motion model is presented on the basis of wave propagation in the two layered half space as the refined wave propagation path and site effect model, and the simple source function which is expressed by the dynamic behaviors of mass-spring system on the rough surface(Ben-Menahem, 1976). This model includes the least physical conditions to characterize the ground motion such as wave propagation from source to site, local site effects and laws governing fault mechanism. The investigation of the basic formation of the characteristics of the ground motion by this simple model will make clear the conditions as to refinements in wave propagation, site effects and source model for a good prediction. Therefore, the verification of this model is developed and the effective key parameters describing the ground motion are investigated through comparison with Miyagi-Oki earthquake, which seems nearly close to a blind prediction test .

2 MIYAGI-OKI EARTHQUAKE DATA

The magnitude of Miyagi-Oki earthquake of June 12, 1978 is reported to be 7.4 by JMA. Table 1. lists the source mechanism parameters for the rupture area which is idealized by the three fault segments(Seno, 1980). Fig.1 shows the geometric relation between those segments and the recording site locations of Ofunato and Shiogama.

3 MODELING OF GROUND MOTION

3.1 Green's function of wave propagation path and site effect model

The propagation spectra of seismic wave motion is considered to be mainly governed with the amplification characteristics of surface soil layer and the multiple scattering characteristics in the heterogeneous earth structure from the source to site(Aki, 1984). So, in this paper, the two layered half space which consists of surface layer overlying a semi-infinite random medium is supposed as the refined wave propagation path and site effect model. The key parameters of the ground motion model are considered to be the ratio of epicentral distance R to focal depth H, the impedance contrast ratio of 1st and

2nd layers, Q values, the fault length and width, the dip angle, the slip direction, the angle between the direction to the recording site and the one of the rupture propagation on the fault surface.

The soil sediment structure of the recording sites of Miyagi-Oki earthquake are reported by many research studies. Table 2. lists the geological data of the soil sediment of Ofunato and Shiogama. The refined wave propagation path and site effect model is presented by the two layered half space shown in Fig. 2(a) using the following equations;

$$\langle V_s \rangle = \frac{\sum_{i=1}^{n} V_{si} H_i}{H}, \quad \langle \rho \rangle = \frac{\sum_{i=1}^{n} \rho_{0i} H_i}{H}$$
$$\langle \nu \rangle = \frac{\sum_{i=1}^{n} \nu_{0i} H_i}{H}, \quad H = \sum_{i=1}^{n} H_i \qquad (1)$$

<A> denotes average of A. H_i, V_{si}, ρ_{0i}, and ν_{0i} are thickness, shear velocity, density, and Poisson's ratio of ith layer of the soil sediment, respectively.

The slip force Q_0 on the fault segment is divided into the two forces Q_H and Q_V as shown in Fig. 2(b). For the estimation of the Green's functions, some discretized points are located on the center line of fault segment. Then, the Green's functions for the forces Q_H and Q_V are calculated exactly according to R/H for each discretized point. Figs. 3 and 4 show some examples of the Green's functions of Ofunato and Shiogama. (HR, HS and HZ) and (VR and VZ) mean the radial, cross-radial and vertical components for the force Q_H, and the radial and vertical components for the force Q_V, respectively.

3.2 Description of source function

The rupture process on the fault surface is reduced to the source function which is expressed by the dynamic behaviors of mass-spring system to stress drop process on the rough surface. The fault segment with length Lf and width Wf is divided into n small elements (of length dL) along the length, called elementary source. The displacement of the rupture propagating from x to $x+dx$ on the fault segment is expressed by (Ben-Menahem, 1976)

$$d(x, a_0) = -\frac{q(x)\Delta x \sin(a_0 T_1)}{Mn\, K(a_0) a_0 T_1} e^{-a_0 \frac{x}{M_n}}$$
$$K(a_0) = (1 - \frac{1}{M_n^2}) a_0^2 - 2ih a_0 + B, \quad T_1 = \frac{\Delta X}{2M_n} \qquad (2)$$

$Mn = Vr/Vs$: Mach number, Vr : rupture velocity, Vs : shear velocity, b : reference length, $a_0 = b\omega/Vs$: nondimensional frequency, B : nondimensional quantity related to shear stiffness of fault surface, $q(x)$: effective force drop
h : damping ratio

An example of the source function is shown in Fig.5, which seems similar to Haskell type model.

Since the time history of stress drop process is unknown, the inverse problem to describe the source function by the information on the stress drop process is solved for only one component N41W of earthquake ground motions observed at Ofunato. The ground motion at ith site is assumed to be expressed by the equation

$$S_i(t) = \sum_{j=1}^{n} q_j S_{eij}(t - t_j) \qquad (3)$$

$S_{eij}(t)$: ground motion at ith site radiated from jth elementary source, q_j : unknown coefficients to be determined by the inversion , t_j : arrival time of rupture front at jth elementary source

To estimate q_j and t_j , the following two equations are used;

$$e_{ti} = \frac{\int_0^t O_i(t) S_i(t) dt}{\sqrt{\int_0^t O_i^2(t) dt} \sqrt{\int_0^t S_i^2(t) dt}}$$
$$e_{mi} = 1 - \frac{\int_0^t \{ 2O_i(t) S_i(t) - S_i^2(t) \} dt}{\int_0^t O_i^2(t) dt} \qquad (4)$$

where $O_i(t)$ is the observed earthquake ground motion. The above first equation is derived by Mellman(1980). The arrival time t_j and q_j are listed in Table 3. q_j is expressed in terms of displacement dimension because it includes the factors for transforming the nondimensional displacement of ground motion to the dimensional one.

3.3 Ground motion

The ground motion is estimated by summation of wave motion radiated at each time when the rupture front reaches at elementary source on the fault segment as follows;

$$Y_D(p; t; r) = \int_0^t \sum_{i=1}^{n} G_D(p; t-\tau; r-r_i) \, n(r_i - \tau) \, d\tau$$
$$n(r, t) = \mu W [d(r, t)]_{,r} \qquad (5)$$

Where μ and $[A]_{,r}$ are shear stiffness of fault surface and derivative of A. $D=(r,s,z)$ and $p(r,s,z)$ denote the com-

ponent of ground motion and the observation location, respectively. In theoretical modeling, to verify the validity of the ground motion by the procedure which seems nearly close to a blind prediction test, the ground motion is expressed by the convolution of the Green's functions of Ofunato and Shiogama and the one source function described above.

4 RESULTS AND DISCUSSION

First, in order to what extent the method presented here could be effective to predict the ground motion, the principal portion of observed motion of Ofunato and the summation of Green's functions radiated at each time when the rupture front reaches at discretized point on the center line of the fault segment are compared in Fig. 6. In this comparison, the two cases (a) and (b) are considered as shown in Fig. 1. Case (a) is corresponding to the reported source locations. In case (b), the location of 2nd fault segment is moved to 10 km West to adjust the energy distribution of N41W and E41N components to that of the observed earthquake. From the above comparison, it is found that the case (b) shows most favorable correspondence in amplitude and phase between them.

Next, the wave form functions of the predicted ground motions are compared with the ones observed at Ofunato and Shiogama as shown in Figs. 7 and 8. In Fig. 7, the principal feature of SH-wave portion of both displacements and velocities of the predicted ground motions are similar to the observed ones. However, they do not have a decreasing coda that is as long in duration as that of the observed earthquake. This is because Q values used to calculate the Green's function of Ofunato is small, and moreover, the high frequency components due to wave scattering at the actual complex boundaries are not so much included in the predicted ground motion. In Fig. 8, the overall features of wave form function are similar to the observed one of Shiogama. From Table 1., the soil sediment of Shiogama has clear strong impedance contrast ratio to the basement, P-wave, SV-wave, and Rayleigh wave portions of the predicted ground motion are similar to those of the observed one. It seems that the soft soil sediment makes markedly amplify the characteristics of the wave motions coming from the basement. Therefore, it is considered that the prediction of the ground motion propagating in the soft soil sediment is relatively easy. A comparison of the predicted and observed Fourier spectra at Ofunato and Shiogama are shown in Figs. 9 and 10, respectively. Fairly good agreement between the predicted and observed Fourier spectra is obtained for both the sites over frequency range of 0.3-3Hz except for the peak in the predicted spectra from 0.1Hz to 0.3 Hz for East component at Shiogama.

5 CONCLUSIONS

For the forward prediction of the ground motion for seismic design, we have presented the simple theoretical ground motion model based on the wave propagation in the two layered half space and source function which is expressed by dynamic behaviors of mass-spring system on the rough surface. The refinements in wave propagation, site effects and source model is investigated for a good prediction of the ground motion. We tested this simple ground motion model against Miyagi-Oki earthquake data of June 12, 1978. The successful agreement is obtained through the comparison of wave form and Fourier spectra functions of the predicted ground motions and observed ones. It is considered that the rigorous estimation of wave propagation from the source to site in the two layered half space play a key role in this successful agreement. It is found that the ratio of epicentral distance to focal depth and the impedance contrast ratio among some selected key parameters are especially important for the forward prediction model of ground motion.

REFERENCES

Seno,T., K. Shimazaki, P. Somerville, K. Kudo and T. Eguchi 1980. Rupture process of the Miyagi-Oki, Japan, earthquake of June 12, 1978. *Phys. Earth. Plant. Interiors* 23: 39-61

Iwan, W. D. 1988. Closure to the special theme session on prediction of strong ground motion. *Proc. 9th WCEE.* 8, SA-C: 89-93

Aki, K. 1984. Prediction of strong motion using physical models of earthquake faulting. *Proc. 8th WCEE.* 2: 433-440

Ben-Menahem, A. 1976. The role of the shear Mach number in earthquake source dynamics. *Bull. S.S.A.* 66: 1787-1799

Mellman, G.R. 1980. A method of body-wave waveform inversion for the determination of earth structure. *Geophys.J.r. astr.Soc.*: 481-504.

Kawano, M. and T. Kobori 1983. Characteristics of earthquake ground motion propagating through the medium with random geological properties. *Trans. of A.I.J.* 330. : 66-77.(in Japanese)

Kawano, M. and T. Kobori 1988. Theoretical modeling of earthquake ground motion and seismic response sensitivity analysis of structural systems. *Proc. 8th WCEE. 8 : 63-68.*(in Japanese)

Kawano, M. 1991. Forward prediction model of earthquake ground motion for seismic design of structural systems o the basis of wave propagation theory and source dynamics. *J. Struct. Constr. Engng. A.I.J.* 424 :105-116.(in Japanese)

Table 1. Source mechanism parameters of Miyagi-Oki earthquake of June 12, 1978

Source Parameters		3 segment model		
		1st seg.	2nd seg.	3rd seg.
Mgnitude		7.4		
Seismic moment	dyn·cm	0.5E27	1.3E27	1.3E27
Strike	deg.	N190E	N160E	N190E
Fault length	km	10	27	24
Fault width	km	17	34	34
Depth of upper edge of fault	km	28	23	38
Dip angle	deg.	20	20	20
Slip direction	deg.	76	76	76
Average slip	m	4.2	2.0	2.3
Rise time	sec	1	2	2
Rupture velocity	km/sec	3.7	3.2	3.2
Shear velocity	km/sec	4.33	4.33	4.33
Stress drop	bar	550	110	135
Time speration between the events	sec	3		8

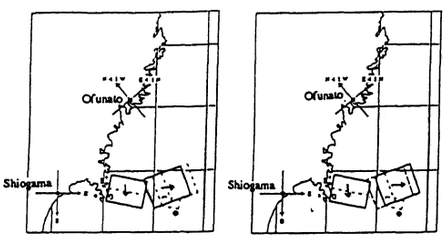

case (a) Case (b)

Fig. 1 Geometric relation between fault segments and recording sites of Ofunato and Shiogama

Table 2. Geological data of soil sediment of Ofunato and Shiogama

Layer	Thickness h(km)	Shear velocity Vs(km/sec)	Density ρ (g/cm^3)	Q	n_i	ρ_{si}	η_i
1st	0.36	1.5	2.3	100	2.4	0.9	0.01
Basement		3.0	2.5	200			

(a) Ofunato

Layer	Thickness h(km)	Shear velocity Vs(km/sec)	Density ρ (g/cm^3)	Q	n_i	ρ_{si}	η_i
1st	0.024	0.08	1.6	8			
2nd	0.003	0.3	1.8	10			
3rd	0.093	0.7	2.0	30	8.3	0.8	0.01
4th	0.08	1.5	2.3	100			
Basement		3.0	2.5	200			

(b) Shiogama

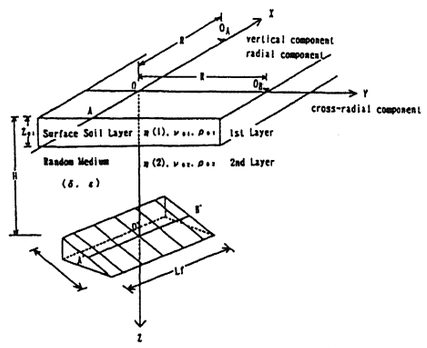

(a) Wave propagation path and site effect model

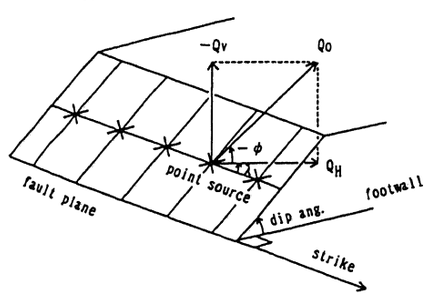

(b) Geometry of fault model

Fig. 2 Wave propagation path and site effect model, and geometry of fault model

Table 3. Arrival time tj and coefficient qj describing source function by inversion of one component of earthquake ground motion observes at Ofunato

	N41W (2nd segment)			N41W (3rd segment)	
	Arrival time tj	Disp. qj		Arrival time tj	Disp. qj
1	−0.10522E+02	0.29735E+01	1	0.32715E+01	0.14849E+01
2	−0.99700E+01	0.34853E+00	2	0.37954E+01	0.76522E+00
3	−0.90520E+01	0.12725E+00	3	0.42930E+01	0.43953E+00
4	−0.85610E+01	0.21211E+01	4	0.51182E+01	0.49926E+00
5	−0.75840E+01	0.26521E+01	5	0.59400E+01	0.14098E+00
6	−0.67460E+01	0.74760E+00	6	0.67599E+01	0.33657E+00
7	−0.61160E+01	0.65969E+00	7	0.72401E+01	0.52058E+00
8	−0.52250E+01	0.22412E+01	8	0.72400E+01	0.0
9	−0.45040E+01	0.73568E+00	9	0.72400E+01	0.0
10	−0.37740E+01	0.11095E+01	10	0.72400E+01	0.0
11	−0.28550E+01	0.53321E+00	11	0.80600E+01	0.98038E−01
12	−0.20630E+01	0.85034E+00	12	0.85001E+01	0.53546E+00
13	−0.10980E+01	0.10710E+01	13	0.93200E+01	0.32865E+00
14	−0.27400E+00	0.79056E−01	14	0.10140E+02	0.30710E+00
15	0.38100E+00	0.81325E+00	15	0.10580E+02	0.57032E+00
			16	0.11240E+02	0.41407E−01
			17	0.11960E+02	0.48688E+00
			18	0.12600E+02	0.80882E+00
			19	0.13420E+02	0.23005E+00
			20	0.14240E+02	0.17265E+00

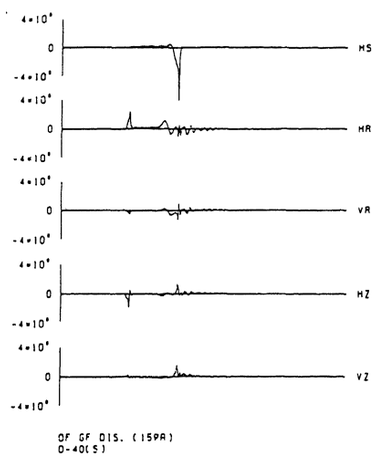

Fig. 3 An example of Green's function of Ofunato

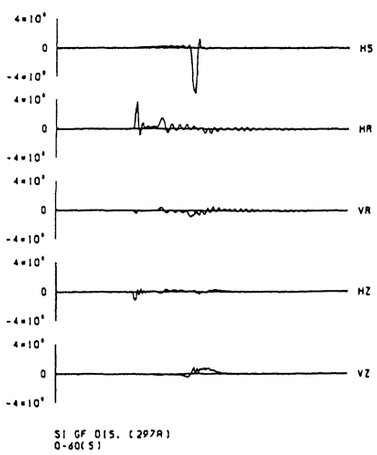

Fig. 4 An example of Green's function of Shiogama

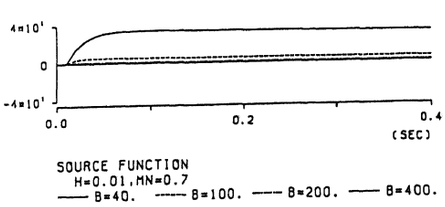

(a) Wave form for *B*

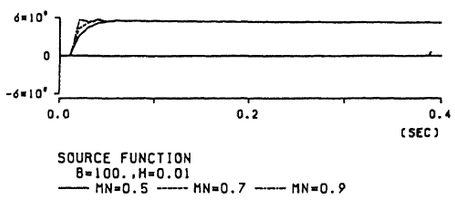

(b) Wave form for *Mn*

Fig. 5 An example of source function

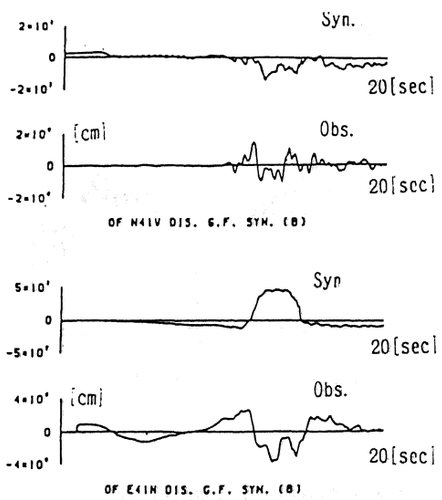

case (a)

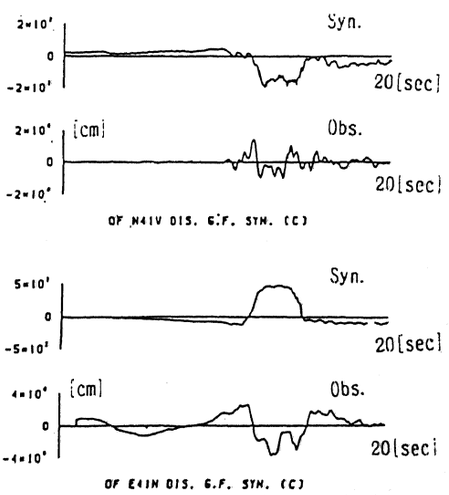

case (b)

Fig. 6 Comparison of principal portion of observed earthquake of Ofunato and summation of corresponding Green's function

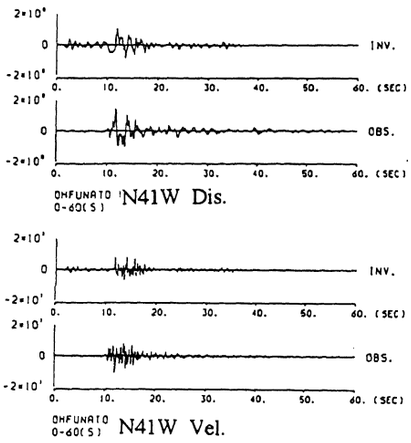

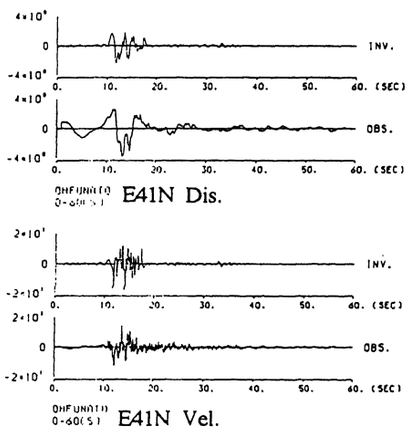

Fig. 7 Comparison of wave form function of predicted ground motion and observed one at Ofunato

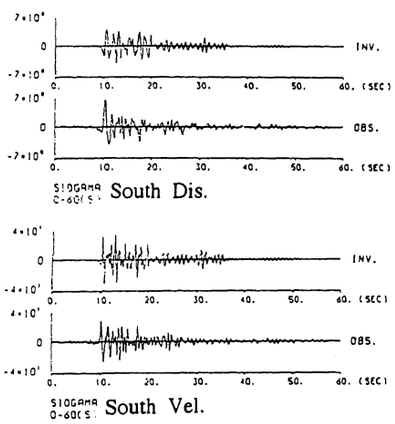

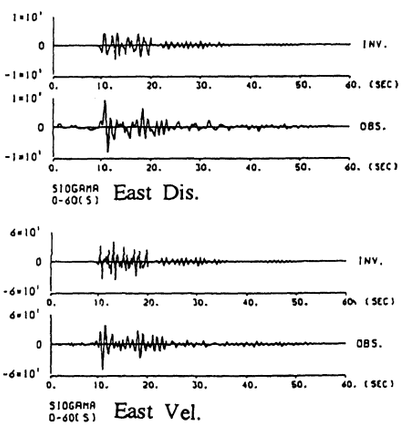

Fig. 8 Comparison of wave form function of predicted ground motion and observed one at Shiogama

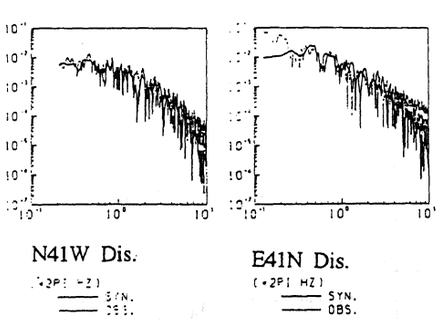

Fig. 9 Comparison of Fourier spectra function of predicted ground motion and observed one at Ofunato

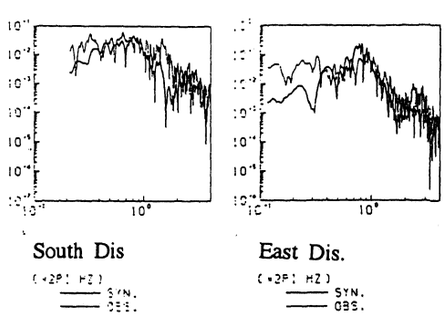

Fig.10 Comparison of Fourier spectra function of predicted ground motion and observed one at Shiogama